Effects of corrosion on the capacity of the nib of reinforced concrete dapped-end beams

Luca Sgambi, Alexandra Bontemps

Louvain research institute for Landscape, Architecture, Built environment (LAB)

Université catholique de Louvain, Belgium

Contact: luca.sgambi@uclouvain.be

Abstract

Many studies have been conducted in the past decades to determine the impact of corrosion on public infrastructures such as bridges, due to the deterioration that has been witnessed since their construction, sometimes very early in their working life. This degradation has caused collapses, not only leading to economic losses but also provoking human casualties. The layout of certain structural elements complicates the inspection and maintenance processes, by creating tight spaces or blocking the access to certain surfaces. This is the case for dapped-end (half-joint) beams, whose height at the extremities has been shortened to create a support, called a nib, reducing the floor height and allowing the placement of an expansion joint. However, water can seep into this joint and stagnate on the lower nib if the drainage system and waterproofing are not adequate. During winter, when de-icing salts are spread on roads, this water becomes charged with chloride ions, which are the leading cause of corrosion in reinforced concrete structures. The purpose of this research is to numerically evaluate this reduction, using a non-linear finite-element analysis that is able to represent an evolving crack pattern taking into account both mechanical degradation due to loading and degradation caused by environmental factors.

Keywords: corrosion; dapped-end beams; durability; nonlinear numerical analysis; finite element modeling.

1 Introduction

A dapped-end beam (DEB), or half-joint beam, is a type of beam frequently used in precast construction, whose section has been reduced at the extremities to create a support, see Figure 1. While this geometry allows for a reduced floor height, easier assembly and a greater lateral stability compared to beams supported at their bottom face [1], it creates a locally disturbed region which relies heavily on its reinforcement to transfer the stress into the full depth of the beam.
The major difference between the stress flow inside the nib of a dapped-end beam and a typical corbel is that while the inclined compression force is transmitted to the column in the case of the corbel, for a DEB this force must be resisted by a tensile force in the vertical reinforcement close to the full-depth face of the beam, as illustrated on Figure 2.
To satisfy equilibrium, this tensile force must be equal to the vertical shear force V acting on the nib. A group of stirrups should be placed close to that interface to resist this component, and be correctly anchored to the longitudinal reinforcement. Two typical reinforcement layouts are presented on Figure 3.
The experiments of Mattock and Chan [1] on DEBs revealed that the nib can be designed as a corbel

if the shear span is taken equal to the distance between the centre of application of the vertical load V and the centre of gravity of the vertical stirrup (also called hanger) reinforcement.

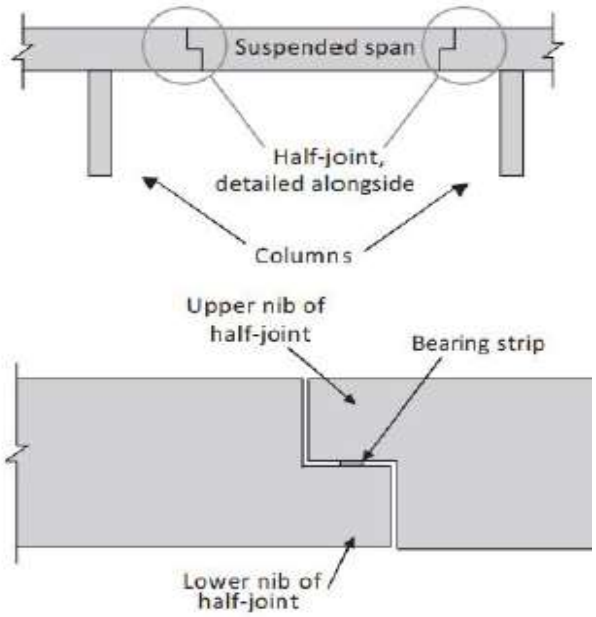


Figure 1. Half-joint principle for reinforced concrete bridges [2]

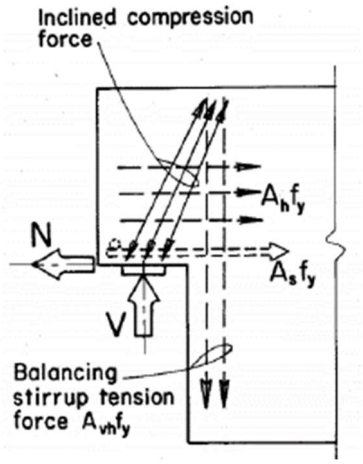


Figure 2. Internal forces for the nib of a dapped-end beam [1]

The cracking process was similar for all the tested specimens, with the first crack initiating at the re-entrant corner at about 20% of the ultimate strength. It propagated at an angle of 45° and extended to two-thirds of the height of the nib at service load. Increasing the load further created additional cracks and lengthened existing ones.

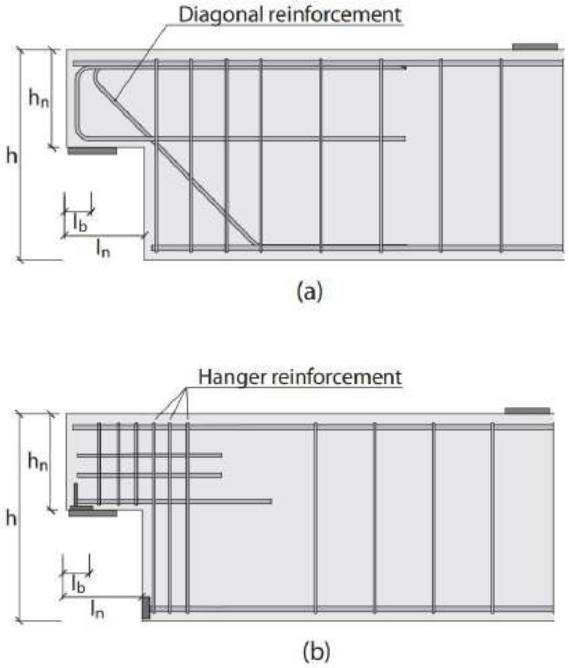


Figure 3. *Typical reinforcement layouts for dapped-end beams : (a) with diagonal reinforcement; (b) without [2]*

As the reinforcement began to yield, the cracks widened significantly and spalling occurred on top of the vertical hanger reinforcement. Right before failure, the same region was subjected to the crushing of the diagonal concrete strut.

In terms of durability, this structural element is subject to two major degradation actions. The first degradation action is a general corrosion of the reinforcements caused by a depassivation of the concrete mass due to the phenomenon of carbonation. In addition to this aspect, common to almost all reinforced concrete structures, there is a local degradation caused by water in the connection joint, which in winter is saturated with de-icing salt.

This research aims to analyze, through a numerical approach, this second type of degradation and its influence on the reduction of the bearing capacity of the structural element. To achieve this goal, a finite element computational code developed by the research group of Prof. Malerba of Politecnico di Milano, with the contribution of one of the authors, was used. The efficiency of this code has already been proven in different publications [3, 4,

5, 6] so in this paper we will only recall some main aspects.

2 Numerical modeling

Since the elastic analysis is not capable of identifying collapse mechanisms depending on the interaction between the concrete matrix and its reinforcement, such as tension stiffening, there is need for a nonlinear formulation. The formulation is base on CFT - MCFT theory, proposed by Vecchio end Collis [7], and implemented for a CST finite elements, coupled with an environmental degradation [6].

2.1 Mathematical formulation of R.C. behavior

A bidimensional membrane constitutive law (CFT, MCFT) [7] has been implemented to study the material nonlinear behavior [8, 9] using a finite element code. In these models, the concrete stiffness matrix is assumed diagonal, in the principal reference system, and its terms are computed using uniaxial laws. The material law is based on a rotating crack model with non-local damage regularization. The uniaxial laws for the compression concrete are reported in the following equations.

If $\varepsilon \le \zeta \cdot \varepsilon_0$:

$$\sigma = \zeta \cdot f'_c \left[2\left(\frac{\varepsilon}{\zeta \cdot \varepsilon_0}\right) - \left(\frac{\varepsilon}{\zeta \cdot \varepsilon_0}\right)^2 \right] \quad (1)$$

Else if $\varepsilon > \zeta \cdot \varepsilon_0$:

$$\sigma = \zeta \cdot f'_c \left[1 - \left(\frac{\frac{\varepsilon}{\zeta \cdot \varepsilon_0} - 1}{\frac{2}{\zeta} - 1} \right)^2 \right] \quad (2)$$

where, the softening parameter ζ, used to reproduce the compression strength in presence of a transversal tensile strain, is evaluated using the following equations:

$$\zeta = \frac{1}{\sqrt{1 + 400 \cdot \varepsilon_{eq}}} \quad (3)$$

$$\varepsilon_{eq} = \sqrt{\langle \varepsilon_1 \rangle^2 + \langle \varepsilon_2 \rangle^2} \quad (4)$$

$$\langle \varepsilon_i \rangle = \begin{cases} \varepsilon_i & \varepsilon_i \ge 0 \\ 0 & \varepsilon_i < 0 \end{cases} \quad (5)$$

Where ε_1 and ε_2 are the strains in the principal directions. The constitutive law for the tensile concrete is:

$$\sigma = E_c \cdot \varepsilon \quad \text{or} \quad \sigma = f_{cr} \left(\frac{\varepsilon_{cr}}{\varepsilon} \right)^{0.4} \quad (6)$$

depending on whether the principal tensile strain is less or more than the cracking strain ε_{cr}.

The constitutive law for the reinforcement steel is assumed elastic - perfectly plastic.

The material stiffness matrix is formed, in the principal reference system, based on the relationships shown. Then, this matrix must be rotated in the Cartesian reference system to allow the assessment of the stiffness matrix of the cracked finite element. For a more in-depth description of the nonlinear mechanical formulation of reinforced concrete, please refer to the previously cited literature papers.

2.2 Mathematical formulation of degradation phenomena

Degradation affects both the concrete and the steel and it is highly dependent on the processes by which the water and the potential aggressive agents (carbon dioxide, chlorides, sulfates, etc.) migrate from the external environment into the concrete mass. These processes are not instantaneous, they occur gradually over a period of time and are influenced by the characteristics of the ambience and by the characteristics of the materials.

The external surfaces of the R.C. elements placed outdoors are exposed to carbon dioxide present the atmosphere, which, interacting with calcium hydroxide of the concrete, gives rise to the carbonation. The exposure conditions may be various, but the carbonation process must be considered always active on any sort of concrete surface in the air.

Another source of damaging is the chloride penetration. Since 1960s, deicing salts have been used in order to make safer the runability of the main roadways during the cold weather. The washing and the percolation of the salted water feed the penetration of chlorides into the concrete mass, frequently fostered by the action of the freezing and thawing cycles. The chloride penetration may surround the whole exposed surfaces or may be localized around some particular sections, as, for instance, those in proximity of the ducts of the drainage system.

Both these phenomena are influenced by the actual state of the concrete surface. A high porosity of the concrete, a low quality of the execution or unfavourable curing conditions accompanied by a wide initial microcracking, stress the propagation phenomena and accelerate the onset of the corrosion. The evolution of these aggressive agents inside the concrete volume can be analyzed through suitable computational models or by analytical equations, corroborated by wide comparisons with the results of experimental tests and of a posteriori controls on bridges in service.

Being mainly interested in the analysis of the mechanical effects of the corrosion, to describe the propagation of the damage causes over time we have used, analytical equations, suitable to deal both with non-cracked and cracked concrete.

The following two paragraphs discuss the formulations used to estimate the depth of carbonation and the critical chloride ion concentration at the rebar surface. A third paragraph will be dedicated to the description of the corrosion evolution model.

2.2.1 Non-cracked concrete

In the case that the concrete is not yet cracked, to model the depth of carbonation we used the of Tuutti's model [10, 11], represented by Eq. 7:

$$x(t) = K \cdot \sqrt{t} \tag{7}$$

Where K is the carbonation coefficient. Instead, the one-dimensional solution of Fick's second law, represented by Eq. 8 and 9 was used to model the chloride concentration present on the surface of the reinforements [12].

$$C(x,t) = C_S \cdot \left[1 - erf\left(\frac{x}{2 \cdot d}\right)\right] \tag{8}$$

$$d = \sqrt{D_{app} \cdot t} \tag{9}$$

Where C_s represents the surface concentration of chloride and D_{app} is the apparent diffusion coefficient of the concrete mass.

2.2.2 Cracked concrete

If cracks appear in the concrete mass, the degradation process is accelerated. In order to consider this aspect, in the finite elements having a main tensile strain greater than the cracking strain, the following equations are considered in place of the previous ones. To calculate the depth of carbonation, the Vesikari equation is used [13]:

$$x(t) = 50 \cdot \sqrt{w} \cdot \sqrt[4]{t} \tag{10}$$

Where w crack width. While for the calculation of the chloride concentration on the rebar surface, the solution of Fick's second law is still used [12, 13] but with an apparent coefficient that depends on the crack width w and their spacing s_{mq}, according to the formulation of Bulfiza [14]:

$$C(x,t) = C_S \cdot \left[1 - erf\left(\frac{x}{2 \cdot d}\right)\right] \tag{11}$$

$$d = \sqrt{D_{app} \cdot t} \tag{12}$$

$$D_{app} = D_{ncrk} + \frac{w}{s_{m\theta}} \cdot D_{crk} \tag{13}$$

Where D_{ncrk} is the diffusion coefficient of non-cracked concrete and D_{crk} is that of cracked concrete.

2.2.3 Corrosion modeling

When the depth of carbonation reaches the reinforcement or when the chloride concentration on the surface of the reinforcement reaches a critical threshold, the so-called "corrosion initiation" period ends and the period called "propagation" begins, with corrosion of the steel bars.
The main consequence of the steel corrosion is a reduction of the sectional area of the bars and, hence, of the bearing capacity of the reinforcement.
Several models are presented in the RILEM Report 14 [14]. The most used gives the effective area of reinforcement , reduced by corrosion, as follows:

$$A_s = \begin{cases} \dfrac{N_s \cdot \pi \cdot D_0^2}{4} & if \quad t \le t_0 \\ \dfrac{N_s \cdot \pi \cdot \left[D_0 - n \cdot d'(t) \right]^2}{4} & if \quad t > t_0 \end{cases} \qquad (14)$$

where:

- N_s is the number of reinforcing bars;
- D_0 is the initial diameter of the reinforcing bar:
- $d'(t)$ is the depth of corrosion;
- t_0 is the time of the corrosion initiation;
- n = (1, 2) is a coefficient which takes into accounts the possibility of the attack coming from one or two sides of the reinforcing bar.

At the time t, the diameter decrease of the corroded reinforcing bar $d'(t)$, which appears in Eq. (14), is estimated through the Faraday's law:

$$d'(t) = 0.0116 \cdot i_{corr} \cdot (t - t_0) \qquad (12)$$

where:

- i_{corr} is the corrosion current per unit area;
- t is the total time since the completion of the building.
- 0.0116 is a conversion factor.

According to this formulation of the Faraday's law and in the case of the steel, to a corrosion current of 1 µA/cm^2 it corresponds a diameter decrease of 11.60 µm/year.

3 Application

The numerical formulation, briefly outlined in the previous section, is used to analyze the decrease in the bearing capacity of a DEB when it is subjected to degradation by carbonation and chloride [16, 17].
The impact of this degradation is evaluated through the reduction of reinforcement diameter and thus ultimate load throughout the years.
Four DEB are investigated, with same geometry but different concrete strength and different cover thickness. Each nib model, called a B-element, will be referred to as BX-Y, with X the concrete strength in [MPa] and Y the cover thickness in [mm]. The selected B-elements are :

- B45-50 : this beam of C45/50 and 50 mm of cover thickness;
- B35-55 : this beam of C35/45 and 55 mm of cover thickness;
- B35-30 : this beam of C35/45 and 30 mm of cover thickness;
- B35-05 : this beam of C35/45 and 5 mm of cover thickness.

These B-elements, were selected to study the repercussions of not following the minimum cover thickness requirement provided by the Eurocode (B35-55 vs B35-30 and B35-05), the reduction in cover thickness that is allowed when using a higher concrete grade (B45-50 vs B35-55) and the consequences of only protecting the reinforcement with a particularly thin cover (B35-05).
Figure 4 shows the dimensions of the DEBs considered and the placement of the main reinforcement. This reinforcement was evaluated using a strut and tie method to have a failure load of about 1000 kN in the absence of environmental degradation.

Each DEB was reinforced with 4D16 in horizontal direction (804 mm^2), 2 vertical closed stirrups D20, spaced by 30 mm (1257 mm^2), 5D16 in diagonal direction (1005mm^2). The steel, considered for these reinforcements, has a yield strength of 500 MPa and an ultimate strength of 650 MPa.

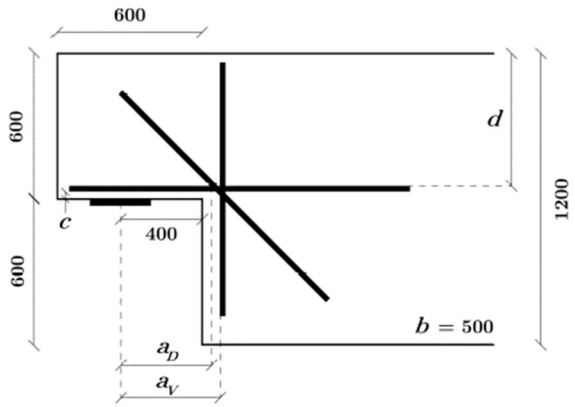


Figure 4. Geometric dimensions and positioning of the main reinforcement in the DEBs investigated

An image of the finite element discretization of a DEB and the placement of the main reinforcement is shown in Figure 5.

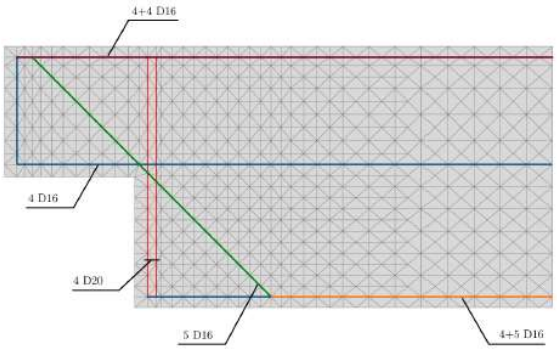


Figure 5. Discretization of a DEB in finite elements

The structural behavior of each DEB has been investigated through 5 nonlinear analyses with increasing load until failure. The first analysis, carried out at initial time (without environmental degradation) shows a collapse load close to the load used in the design phase with the strut and tie method (between 900 and 1000 kN for all DEBs). The other analyses were performed by simulating environmental degradation caused by carbonation and chloride, with exposures of 20, 40, 60, and 80 years.

Figure 6 shows a crack pattern for one of the analyses performed, in a loading situation close to the collapse load.

We can see the formation of a 45-degree crack region at the re-entrant corner of the DEB and an area of bending moment cracking to the right of it.

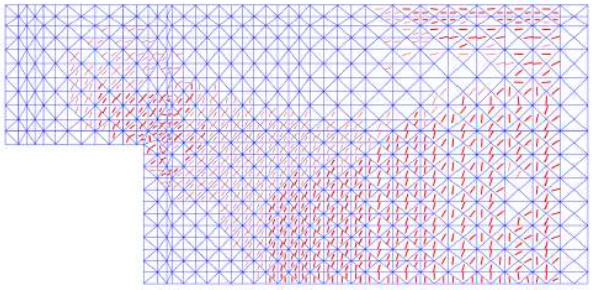


Figure 6. Internal forces for the nib of a dapped-end beam

Figure 7 and Figure 8 show the decrease in collapse load over time for the four case studies considered. Figure 7 is for simulations with environmental degradation caused by a surface concentration of 0.2% chloride, while Figure 8 considers a surface concentration of 1%.

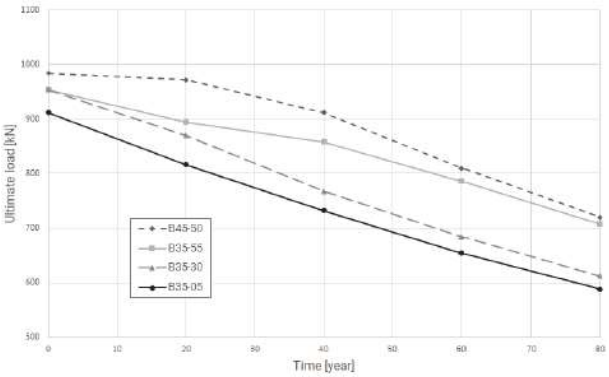


Figure 7. Reduction of the ultimate load in time with C_S = 0.2%

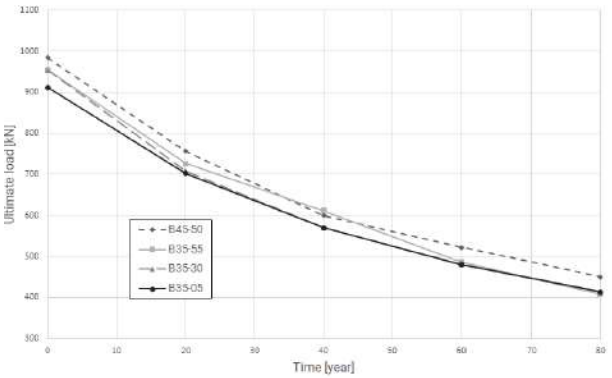


Figure 8. Reduction of the ultimate load in time for with C_S = 1%

4 Conclusions

This research aims to analyze the collapse strength of DEBs subjected to environmental

degradation caused by carbonation and chloride ions. Four different DEBs are considered, having different concrete qualities and different concrete cover values. Each element is analyzed using a nonlinear finite element calculation code capable of taking into account the reduction of the steel section of the reinforcing bars in relation to the life time of the structure and the concentrations of degrading substances present in the environment. From the results of the numerical analysis, the following points can be highlighted:

- The protective nature of a proper cover thickness against the corrosion of the steel reinforcement is demonstrated once again. The comparison between the crack opening widths of the elements also evokes the negative influence of using a thicker cover on the cracking.
- For C_s = 0.2% (Figure 7), there is a marked difference between the B-elements throughout the years, with again the thicker covers retaining the highest final load-carrying capacities. For C_s = 1% (Figure 8), the reduction follows a similar slope for every element. Their final load is almost identical apart from B45-50, for which it is slightly higher. This suggests that the cover thickness does not play much of a protective role for such a high chloride surface content.
- B35-30 and B35-05 have very similar degradation rates, hinting at the fact that a cover depth below a certain value does not offer significant protection anymore. We can note that their thicknesses are both well under the minimal requirements of the Eurocode.
- If failure is deemed to happen as soon as the load reduction reaches 40%, all elements reach their ultimate state before 50 years for C_s = 1%. For C_s = 0.2%, B45-50 and B35-55, possessing the highest covers, attain roughly 40% of reduction at 80 years, while the others fail sooner.
- The re-entrant corner is critical for the durability and load-carrying capacity of the nib of the dapped-end beam. In the case of the lower nib, water can penetrate inside the major diagonal crack rapidly through gravity. If the water is charged with chloride ions, the degradation begins very quickly. Since the nib is the part of the beam subjected to the highest shear stress, due to being at the support, it is crucial for the reinforcement to be able to sustain the loading applied on the structure for the entirety of the chosen working life.

The results obtained are clearly subject to many limitations, as only a numerical analysis was performed. In particular, in addition to the usual limitations resulting from modeling the nonlinear behavior of reinforced concrete, other limitations are also present for modeling degradation parameters.

5 References

[1] Mattock A.H. and Chan T.C. Design and Behavior of Dapped-End Beams, *PCI Journal*. 1979; **24**(6): 28–45.

[2] Desnerck P. and Lees J.M. Impact of the reinforcement layout on the load capacity of reinforced concrete half-joints, *Engineering Structures*. 2016; **127**: 227–239.

[3] Gotti G., Ielmini D., Malerba P.G. and Sgambi L. Influenza dei fenomeni di corrosione sulla modalità di rottura di elementi strutturali in calcestruzzo armato precompresso. *Proceedings of the Handling Exceptions in Structural Engineering*, Rome, 8-9 July 2010.

[4] Malerba P.G., Sgambi L., Ielmini D. and Gotti G. Influence of Corrosive Phenomena on the mechanical behaviour of R.C. Elements. *Proceedings of the 2011 World Congress on Advances in Structural Engineering and Mechanics*. Seoul, Korea, 18-22 September 2011

[5] Sgambi L., Malerba P.G., Gotti G. and Ielmini D. The influence of degradation phenomena on collapse modes in prestressed concrete beams. *International Journal of Lifecycle Performance Engineering*. 2012; **1**(1), 41-63.

[6] Malerba P.G., Sgambi L., Ielmini D. and Gotti G. Influence of corrosive phenomena on bearing capacity of RC and PC beams, *Advances in Concrete Construction*. 2017; **5**(2): 117 – 143.

[7] Vecchio F.J. and Collins M.P.C. The Modified Compression-Field Theory for Reinforced Concrete Elements Subjected to Shear, *ACI Structural Journal*. 1986; **83**(2): 219-231.

[8] Sgambi L. Fuzzy theory based approach for three-dimensional nonlinear analysis of reinforced concrete two-blade bridge piers. *Computers and Structures*. 2004; **82**(13-14), 1067-1076.

[9] Garavaglia E., Pizzigoni A., Sgambi L. and Basso N. Collapse behaviour in reciprocal frame structures, *Structural Engineering and Mechanics*. 2013; **46**(4): 533 – 547.

[10] Tuutti K. Corrosion of Steel in Concrete, *CBI Research Report*. 1982; no. 4.82, Swedish Foundation for Concrete Research, Stockholm, Sweden.

[11] Bertolini L., Elsener B., Pedeferri P. and Polder R.P. Corrosion of Steel in *Concrete: Prevention, Diagnosis, Repair*. 2004; WILEY-VCH Verlag GmbH & Co. KGaA, Weinheim.

[12] Vidal T., Castel A. and François R. (2007). Corrosion process and structural performance of a 17 year old reinforced concrete beam stored in chloride environment, *Cement and Concrete Research*. 2007; **37**(11): 1551-1561.

[13] Vesikari E. Service life prediction of concrete structures with regard to corrosion of reinforcement. *Research Report* NA 553, 1988; Technical Research Center of Finland (VTT), Finland.

[14] Sarja A. and Vesikari E. Durability Design of Concrete Structures, RILEM Report Series 14. 1996; RILEM Technical Committee 130-CSL, E & FN Spon, London.

[15] Boulfiza M., Sakai K., Banthia N. and Yoshida H. Prediction of Chloride Ions Ingress in Uncracked and Cracked Concrete, *ACI Materials Journal*. 2003; **100**(1), 38-48.

[16] Sarveswaran V., Roberts M., and Anstice O. Reliability assessment of deteriorating RC bridge half joints. In: *Proceedings of the 25th conference on our world in concrete and structures*, Singapore : CI-Premier PTE Ltd, 2000, pp. 555–562.

[17] Santhanam B. and Shah P. Concrete half joint bridges in New South Wales: challenges in risk management. In: *Austroads Bridge Conference*, Sydney, 2011, pp. 497–511.